Conventional vs Unconventional Magnetic Polarons: ZnMnTe/ZnSe and ZnTe/ZnMnSe Quantum Dots

B. Barman[a], Y. Tsai[a], T.Scrace[a], J.R.Murphy[a], A.N.Cartwright[a], J. M. Pientka[a], I.Zutic[a], B.D. McCombe[a], and A. Petrou[a], I. R. Sellers[b], R.Oszwaldowski[c], A.Petukhov[c], W.C.Fan[d], W.C.Chou[d], C.S. Yang[e]
[a]University at Buffalo, The State University of New York, 12 Capen Hall, Buffalo, NY 14260
[b]University of Oklahoma, 660 Parrington Oval, Norman, OK 73019
[c]South Dakota School of Mines and Technology, 501 E St Joseph St, Rapid City, SD 57701
[d]National Chiao Tung University, 1001 University Road, Hsinchu, Taiwan 300
[e]Graduate Institute of Electro-Optical Engineering, Tatung University, 40 Zhongshan North Road, 3rd Section Taipei 104, Taiwan

ABSTRACT

We used time resolved photoluminescence (TRPL) spectroscopy to compare the properties of magnetic polarons in two related, spatially indirect, II-VI epitaxially grown quantum dot systems. In sample A (ZnMnTe/ZnSe), the photo-excited holes are confined in the magnetic ZnMnTe quantum dots (QDs), while the electrons remain in the surrounding non-magnetic ZnSe matrix. In sample B (ZnTe/ZnMnSe) on the other hand, the holes are confined in the non-magnetic ZnTe QDs and the electrons move in the magnetic ZnMnSe matrix. The magnetic polaron formation energies, E_{MP}, in these samples were measured from the temporal red-shift of the excitonic emission peak. The magnetic polarons in the two samples exhibit distinct characteristics. In sample A, the magnetic polaron is strongly bound with $E_{\mathrm{MP}} = 35$ meV. Furthermore, E_{MP} has unconventionally weak dependence of on both temperature T and magnetic field B_{appl}. In contrast, magnetic polarons in sample B show conventional characteristics with E_{MP} decreasing with increasing temperature and increasing external magnetic field. We attribute the difference in magnetic polaron properties between the two types of QDs to the difference in the location of the Mn ions in the respective structures.

Keywords: magnetic quantum dots, magnetic polaron dynamics, exchange interaction

1. INTRODUCTION

The presence of magnetic ions such as Mn^{+2} in semiconductor structures allows the formation of magnetic polarons (MP)[1, 2] due to exchange interactions between the magnetic ion spin and spins of photo-excited electrons and the holes[3]. This interaction tends to align the Mn^{+2} - hole (Mn^{+2}- electron) spins antiferromagnetically (ferromagnetically), and results in a reduction of the energy of carrier- Mn^{+2} complex known as the "magnetic polaron". Magnetic polaron (MP) dynamics have been studied using time-resolved (TR-PL) photoluminescence spectroscopy in two classes of magnetic quantum dot (QDs) ensembles: The first class is grown by molecular beam epitaxy (MBE) in CdSe/ZnMnSe[4] and CdSe/ZnMnSe[5] quantum dots. The samples in both studies are spatially direct (type-I) and have the magnetic ions in the barriers, while the photo-excited carriers remain in the non-magnetic quantum dots. The observed magnetic polarons have low binding energy ($E_{\mathrm{MP}} = 21$ meV at $T = 6$ K in Ref 4 and $E_{\mathrm{MP}} = 15$ meV at $T = 5$ K in Ref 5). In addition, the binding energy of the magnetic polarons in Ref 5 decreases rapidly with increasing temperature ($E_{\mathrm{MP}} = 9$ meV at $T = 21$ K). This is not surprising since the excitons in the quantum dots are spatially segregated from the magnetic ions in the barriers. The second class are solution processed magnetic quantum dots, known as colloidal quantum dots. References 13 and 14 describe a study of spatially direct CdMnSe QDs. The magnetic polarons in this system are robust with $E_{\mathrm{MP}} = 68$ meV and a weak temperature dependence. These properties have been attributed to the fact that the electrons and holes are confined in the same space as the Mn ions.

Spintronics VII, edited by Henri-Jean Drouhin, Jean-Eric Wegrowe, Manijeh Razeghi, Proc. of SPIE
Vol. 9167, 91670L · © 2014 SPIE · CCC code: 0277-786X/14/$18 · doi: 10.1117/12.2064339

In this work we compare two spatially indirect (type-II) MBE grown QD structures based on the ZnTe/ZnSe system[6]. In sample A (ZnMnTe/ZnSe) the Mn^{+2} ions are located in the quantum dots; in sample B (ZnTe/ZnMnSe) the Mn^{+2} ions are in the barriers. The comparison of the MP properties in these two samples allows us to investigate the influence of the location of the magnetic ions within the QD structure. The ZnTe/ZnSe system offers the following advantages: a) The spatially indirect character of the band structure results in long recombination times (several nanoseconds), allowing for full development of magnetic polarons, whose formation times are typically around 0.5 ns, b) the interband transition energy is 1.9 eV which is lower than the energy of the competing Mn^{+2} internal transition at 2.2 eV[3]. As a result, the lower energy interband transition dominates the emission spectra. The formation of magnetic polarons is observed in both samples. In sample A, the polaron is robust with a formation energy E_{MP} which is insensitive to increase in temperature and the application of an external magnetic field. In contrast, E_{MP} in sample B decreases with increasing temperature and increasing magnetic field.

2. EXPERIMENTAL

Schematic diagrams of the band structure of sample A and sample B are shown in Fig. 1a and Fig. 1b, respectively. The shaded areas represent the location of the Mn^{+2} in the samples. The conduction (valence) band offset is 0.6 (1.0 eV) resulting in a spatially indirect (type-II) system. In sample A (sample B), the holes are confined in the ZnMnTe (ZnTe) quantum dot, while the electrons orbit around the quantum dot in the ZnSe (ZnMnSe) matrix held by the electron-hole coulomb interaction. Both samples were grown by molecular beam epitaxy (MBE) on (100) GaAs substrate; the details on growth were given elsewhere[7, 8]. The quantum dots are disk-shaped with 20 nm average diameter and 3 nm average height. The average Mn molar composition of the ZnMnTe QDs in sample A and the ZnMnSe barriers in sample B was determined to be 5.2 % using Energy Dispersive X-Ray Spectroscopy. Together with

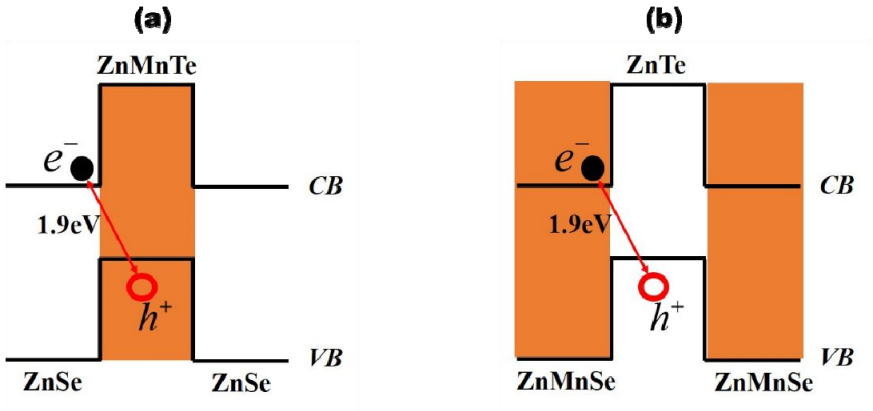

Fig. 1: Schematics of the band alignment in (a) ZnMnTe/ZnSe (b) ZnTe/ZnMnSe

sample A and sample B we also studied the properties of corresponding non-magnetic references as will be discussed below. The interband transitions occur at 1.9 eV. In the Faraday geometry spin -1/2 (+1/2) electrons recombine with +3/2 (-3/2) holes and emit light which is circularly polarized as σ_+ (σ_-). The samples were placed in a variable temperature optical magnet cryostat and the PL was excited at 400 nm by a frequency doubled pulsed laser system, which emits at 800 nm (repetition rate = 250 kHz, pulse duration ~200 fs). The external magnetic field was applied along the direction perpendicular to the QD layers, defined as the *z*-axis. The emitted luminescence was spectrally resolved by a monochromator, and temporally analyzed by a streak camera having a temporal resolution of 40 ps. A combination of quarter-wave plate and linear polarizer was placed in appropriate configurations before the spectrometer entrance slit to separate the σ_+ from the σ_- components of the emission spectra.

3. RESULTS AND DISCUSSION

The output of the streak camera for sample A at $T = 7$ K is shown in Fig. 2 at zero applied magnetic field. The horizontal axis corresponds to the PL energy, while the vertical axis represents the PL time evolution. The PL intensities are represented by the color scale shown in the figure. The exciting laser pulse arrived at $t = 1.96$ ns for these data. The

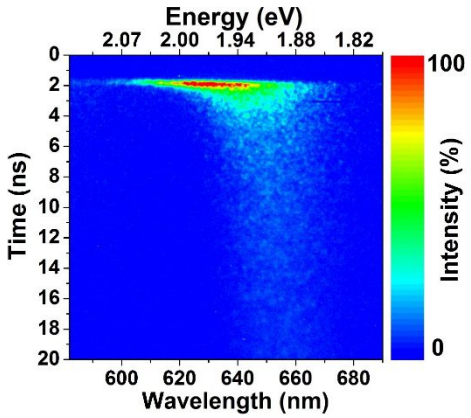

Fig. 2: Output of the streak camera used in our experiments. The horizontal axis corresponds to PL photon energy. The vertical axis represents the time evolution of PL energy

time at which photon collection starts was chosen to be earlier than the pulse arrival to ensure that the entire PL time evolution was recorded. The time delay Δt in the remainder of the text is defined as the difference between the detection time and the pulse arrival time (i.e. difference between the detection time and the photon-collection start time in Fig. 2). In Fig.3a (Fig. 3b), we plot the zero field PL peak energy as function of Δt for sample A and its non-magnetic reference (sample B and its non-magnetic reference). Immediately after the pulse arrival, the PL peak energies red-shift with increasing time delay, for all four samples.

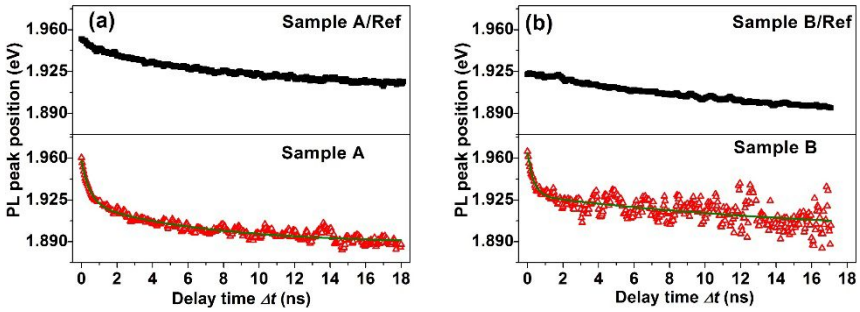

Fig. 3: PL peak energies as function of time delay. (a) Upper panel: Non-magnetic reference for sample A; Lower panel: Sample A (b) Upper panel: Non-magnetic reference for sample B; Lower panel: Sample B

For the laser powers used in our experiments, the peak energy of the non-magnetic reference samples exhibit a smaller but sizeable red shift, as shown in the upper panels of Fig. 3a and Fig. 3b, which is well fitted by a single exponential time evolution. The corresponding time constants τ_{slow} are given in Table 1 at $T = 7$ K and $B_{appl} = 0$. In order to obtain a comparable quality fit for the magnetic samples A and B [green lines in Fig. 3a and Fig. 3b, respectively], the TR-PL peak position requires the use of two decaying exponentials with two corresponding time constants; a fast time constant τ_{fast} below 1 ns, and a slower time τ_{slow}, which is comparable to τ_{slow} of the non-magnetic references. Given the similarity of the two slow time scales between the magnetic samples and their non-magnetic references, we attribute the entire red shift of the peak position in non-magnetic reference samples and the red shift of

the slower component in magnetic samples A and B to the same spin-independent mechanism: electric-dipole layer formation at the wetting layer/matrix interface. Such dipole layers have been predicted and studied by other groups [9, 10]. The fitted fast and slow time constants for samples A and B are also given in Table 1. The total temporal red shift R of the TR-PL for the magnetic samples A and B is defined as the sum of the two energy parameters in the bi-exponential fit of the peak position energy described above. Even though the red shifts R of the two magnetic samples, and the red shifts R_{ref} of the non-magnetic reference samples depend strongly on laser power, the difference $E_{MP} = R - R_{ref}$ remains constant over a wide range of laser powers, indicating that E_{MP} is not related to dipole layer formation. We attribute the faster component τ_{fast} of the red shifts in the magnetic samples A and B to the formation of magnetic polarons and identify τ_{fast} as the MP formation time τ_{MP}. The MP formation produces a temporal red shift as shown in Fig. 3 under the following assumptions: (a) The hole-spin quantization axis is perpendicular to the QD plane due to the large shape anisotropy and spin-orbit interaction [11, 12] (b) Following electron and hole photo-injection, MPs are formed; (c) The Mn-hole exchange interaction is 5 times larger than the Mn-electron exchange interaction [3]. Therefore, the influence of electrons on MP formation for sample A can be neglected, especially since the electron wavefunction overlap with the Mn ions, is much smaller than those of the holes. This is not the case for sample B for which we have the opposite situation i.e. large electron-Mn and small hole-Mn wavefunction overlap.

Table 1: Fitting parameters for the TR-PL of the samples used in this study

Sample	τ_{fast} (ns)	τ_{slow} (ns)	E_{MP} (meV)
A	0.60	9.0	35.3
Reference of A	X	6.9	X
B	0.35	17	25.4
Reference of B	X	16	X

The TR-PL peak at $\Delta t = 0$ corresponds to the exciton recombination energy prior to the alignment of the Mn spins with the spins of the carriers i.e. prior to the MP formation. A schematic of the valence band of sample A and sample B is given in Fig. 4a and Fig. 4b, respectively, at zero magnetic field.

Just after photo-excitation ["early times", upper row Fig. 4] the average spin of the Mn ions in the z-direction is zero, and the two hole spin states ($m_J = \pm 3/2$) in a given QD are degenerate. The hole spins are indicated in Fig. 4 by open red arrows. At later times (lower row in Fig.4) the exchange interaction between the spins of carriers and the Mn^{+2} spins (The Mn^{+2} spins are indicated by orange arrows) aligns the latter antiparallel with the hole spins and parallel to the electron spins. This leads to the formation of the magnetic polaron and the overall reduction of system's energy by E_{MP}.

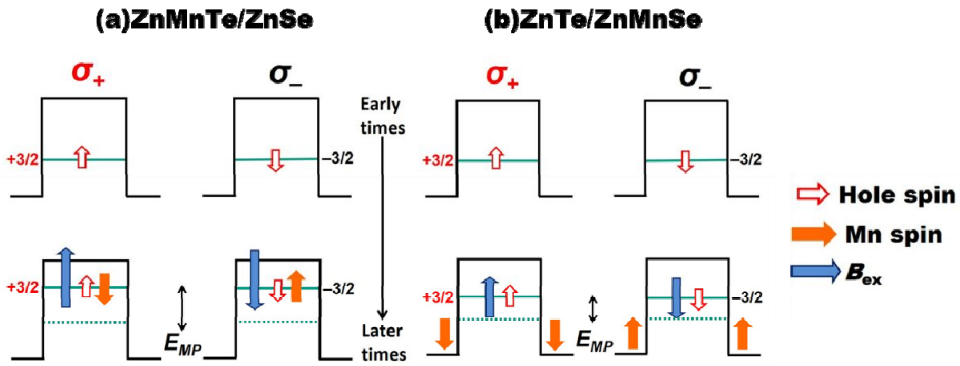

Fig. 4: Schematic diagram of the MP formation at zero magnetic field (a) in ZnMnTe/ZnSe QDs (b) in ZnTe/ZnMnSe QDs

The hole-Mn exchange interaction can be described also by an exchange magnetic field B_{ex} (which can be much stronger than an externally applied field B_{appl}) exerted by the hole spin on the Mn spins within the hole wavefunction[13]. The exchange field is indicated in Fig.4 by blue arrows. In both samples at later times, the overall energy of the system is reduced by E_{MP} with a time constant τ_{MP} . From Table 1 it is clear that E_{MP} is larger in sample A than in sample B at $T = 7$ K and $B_{appl} = 0$. This is attributed to the fact that in sample A the Mn and the holes are confined in the same space (the ZnMnTe QDs); in contrast, in sample B the Mn spins are located outside the ZnTe quantum dots resulting in a weaker exchange interaction. In sample A, the main contribution to E_{MP} comes from the Mn-hole exchange. In sample B, both the hole-Mn and the electron-Mn exchange contribute.

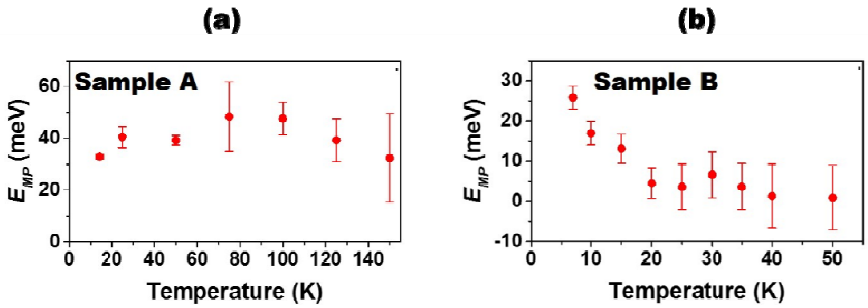

Fig. 5: Magnetic polaron formation energy at zero magnetic field plotted as a function of temperature (a) Sample A (b) Sample B

The magnetic polaron energies for zero magnetic field are plotted as function of temperature in Fig. 5a and Fig. 5b for samples A and B, respectively. The magnetic polaron energy E_{MP} of sample B shows a "conventional" temperature dependence, i.e., it decreases with increasing temperature[5]. In contrast, E_{MP} of sample A has a weak dependence on T .

We also observe that E_{MP} in samples A and B have distinct dependences on magnetic field B_{appl} when temperature is held constant at $T = 7$ K , see Fig. 6. Again, sample B exhibits the conventional trend i.e. E_{MP} decreases with increasing applied magnetic field B_{appl} . In contrast, E_{MP} in sample A is roughly independent of magnetic field.

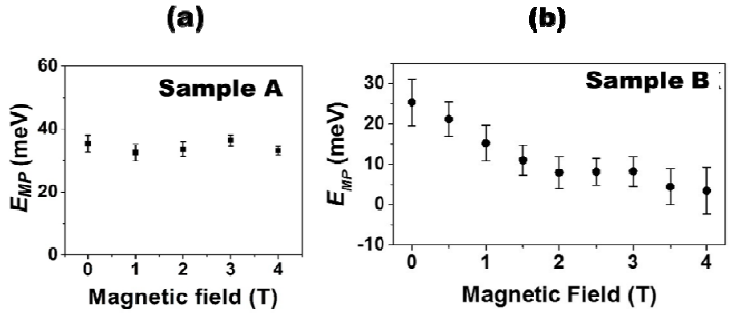

Fig. 6: Magnetic polaron formation energy at T=7 K plotted as a function of magnetic field (a) Sample A (b) Sample B

We attribute these striking differences between sample A and sample B to distinct Mn magnetic susceptibilities χ in the two samples.

The magnetic polaron energy is given by the equation[1]:

$$E_{\mathrm{MP}} = \mu_0^{-1}\left(J_{ex}/2g\mu_B N_0\right)^2 \eta\left(E_{\mathrm{MP}}/k_B T\right)\Omega_{eff}^{-1}\chi(T) \quad \text{(eqs.1)}$$

where J_{ex} is the exchange integral for carriers, N_0 is the cation density, $g = 2$, μ_B is the Bohr magneton, and Ω_{eff} is the effective volume of the magnetic polaron. The term $\eta\left(E_{\mathrm{MP}}/k_B T\right) = \tanh\left(E_{\mathrm{MP}}/k_B T\right)$ [14].

Sample B is characterized by conventional paramagnetic susceptibility, which decreases quickly with temperature. Based on eqs.1, the strongly temperature dependent χ explains the trend in Fig. 5b. At the same time, the conventional values of χ at low temperatures are sufficiently high to allow for significant alignment of Mn spins in the presence of an applied magnetic field of a few tesla. Due to this alignment, the temporal red-shift of PL, identified as the magnetic polaron formation energy E_{MP}, is smaller than that for $B_{appl} = 0$. This is because recombination events at zero delay time occur for hole energies corresponding to partially aligned Mn spins, while events at long delay times occur for full alignment, as they did for zero magnetic field. Therefore, the energy difference between zero-delay and long delay recombination events (i.e. E_{MP}) must be smaller than the same difference at $B_{appl} = 0$, in agreement with the results of Fig. 6b.

Applying the above approach to sample A, we attribute the trends in Fig. 5a and Fig. 6a to an unconventional magnetic susceptibility of the Mn spins. Presently, it is not clear what determines χ in sample A. One possibility is the spatial anisotropy of the ZnMnTe QDs. This viewpoint is compatible with the bulk-like susceptibility of Mn uniformly distributed in the ZnMnSe barrier of sample B. Further effort to explain the behavior of χ in sample A will use ZnMnTe/ZnSe structures with different Manganese compositions (both below and above 5.2 %).

ACKNOWLEDGEMENT

This work is supported by DOE-BES DE-SC0004890 and NSF DMR-1305770.

REFERENCES

[1] Dietl, T., and Spalek, J., "Effect of Fluctuations of Magnetization on the Bound Magnetic Polaron - Comparison with Experiment," Physical Review Letters, 48(5), 355-358 (1982).

[2] Kossut, J., and Gaj, J. A., [Introduction to the physics of diluted magnetic semiconductors] Springer Verlag, Heidelberg ; New York(2010).

[3] Furdyna, J. K., "Diluted Magnetic Semiconductors," Journal of Applied Physics, 64(4), R29-R64 (1988).

[4] Dorozhkin, P. S., Kulakovskii, V. D., Chernenko, A. V., Brichkin, A. S., Ivanov, S. V., and Toropov, A. A., "Controlling magnetic moment and its fluctuations in individual semimagnetic quantum dots with different exchange interactions," Applied Physics Letters, 86(6), (2005).

[5] Seufert, J., Bacher, G., Scheibner, M., Forchel, A., Lee, S., Dobrowolska, M., and Furdyna, J. K., "Dynamical spin response in semimagnetic quantum dots," Physical Review Letters, 88(2), (2002).

[6] Yang, C. S., Lai, Y. J., Chou, W. C., Chen, W. K., Lee, M. C., Kuo, M. C., Lee, J., Shen, J. L., Jang, D. J., and Cheng, Y. C., "Optical properties of self-assembled ZnTe quantum dots grown by molecular-beam epitaxy," Journal of Applied Physics, 97(3), (2005).

[7] Kuo, M. C., Hsu, J. S., Shen, J. L., Chiu, K. C., Fan, W. C., Lin, Y. C., Chia, C. H., Chou, W. C., Yasar, M., Mallory, R., Petrou, A., and Luo, H., "Photoluminescence studies of type-II diluted magnetic semiconductor ZnMnTe/ZnSe quantum dots," Applied Physics Letters, 89(26), (2006).

[8] Lee, L., Fan, W. C., Chien, K. F., Tzou, A. J., and Chou, W. C., "Growth evolution and magneto-optical characteristics of self-assembled ZnTe/ZnMnSe quantum dots," Journal of Crystal Growth, 378, 222-225 (2013).

[9] Gu, Y., Kuskovsky, I. L., van der Voort, M., Neumark, G. F., Zhou, X., and Tamargo, M. C., "Zn-Se-Te multilayers with submonolayer quantities of Te: Type-II quantum structures and isoelectronic centers," Physical Review B, 71(4), (2005).
[10] Ledentsov, N. N., Bohrer, J., Beer, M., Heinrichsdorff, F., Grundmann, M., and Bimberg, D., "Radiative States in Type-Ii Gasb/Gaas Quantum-Wells," Physical Review B, 52(19), 14058-14066 (1995).
[11] Klopotowski, L., Cywinski, L., Wojnar, P., Voliotis, V., Fronc, K., Kazimierczuk, T., Golnik, A., Ravaro, M., Grousson, R., Karczewski, G., and Wojtowicz, T., "Magnetic polaron formation and exciton spin relaxation in single Cd1-xMnxTe quantum dots," Physical Review B, 83(8), (2011).
[12] Vyborny, K., Han, J. E., Oszwaldowski, R., Zutic, I., and Petukhov, A. G., "Magnetic anisotropies of quantum dots doped with magnetic ions," Physical Review B, 85(15), (2012).
[13] Beaulac, R., Schneider, L., Archer, P. I., Bacher, G., and Gamelin, D. R., "Light-Induced Spontaneous Magnetization in Doped Colloidal Quantum Dots," Science, 325(5943), 973-976 (2009).
[14] Sellers, I. R., Oszwaldowski, R., Whiteside, V. R., Eginligil, M., Petrou, A., Zutic, I., Chou, W. C., Fan, W. C., Petukhov, A. G., Kim, S. J., Cartwright, A. N., and McCombe, B. D., "Robust magnetic polarons in type-II (Zn, Mn) Te/ZnSe magnetic quantum dots," Physical Review B, 82(19), (2010).